Chalcogenide Letters Vol. 11, No. 11, November 2014, p. 611 - 618

OPTICAL AND MORPHOLOGICAL INVESTIGATIONS OF THERMALLY VACUUM EVAPORATED ZnTe THIN FILMS

O. TOMA[a], S. ANTOHE[a,b*]
[a]*University of Bucharest, Faculty of Physics, 405 Atomistilor Street, PO Box MG-11, 077125, Magurele-Ilfov, Romania*
[b]*Academy of Romanian Scientists, 54 Splaiul Independent_ei, Bucharest, Romania*

Zinc telluride p-type semiconductor thin films were deposited onto optical glass substrates using thermal vacuum evaporation (TVE) technique. During the deposition, the evaporation source (a single quartz crucible) was maintained at a temperature of 550° C while substrates were heated at 230° C. All the zinc telluride thin films were subjected to a post-deposition thermal treatment in the same deposition chamber at temperatures of 250° C for 20 minutes. Optical constants (refractive index and extinction coefficient) as well as transmission and absorption spectra were computed using the spectroscopic ellipsometry technique. From absorption spectra the optical band gap of ZnTe thin films was computed. Morphological characterizations were made by AFM and SEM and the influence of the post-deposition thermal treatments on the grains distribution over the film surfaces was discussed.

(Received October 10, 2014; Accepted November 29, 2014)

Keywords: zinc telluride, spectroscopic ellipsometry, AFM, SEM

1. Introduction

From $A_{II} – B_{VI}$ binary semiconductor compounds, zinc telluride (ZnTe) thin films are widely used in manufacturing different solid-state optoelectronic devices (photodetectors, solar cells, light-emitting diodes, laser diodes, microwave devices, etc.) due to its specific optical and electrical properties (relatively wide direct optical band gap, high transparency in visible and infrared regions, low electrical resistivity, etc.) [1 – 5].

ZnTe thin films have been prepared by different techniques, including pulsed laser deposition (PLD) [6], magnetron sputtering [7], thermal evaporation [8 – 10], molecular beam epitaxy (MBE) [11], electron beam [12], closed space sublimation (CSS) [13], electro-deposition [14], etc.

More recently, p-type semiconductor ZnTe thin films were also used in photovoltaic technologies as high efficiency stable back contacts for CdTe thin films based solar cells [15 – 17]. As it is known, the CdTe solar cells are rapidly growing in the photovoltaic market because of CdTe optimum band gap (1.45 eV) and its high optical absorption coefficient (10^5 cm^{-1} in visible range) [18].

However, the need for higher efficiencies of CdTe solar cells [19] is facing some challenging points including the back contact (among the needs for high-transparency windows, low recombination and optical losses, low-defect density junction, etc.). Forming low resistance ohmic back contacts is difficult due to CdTe high work function (5.9 eV) and this is the reason why the method of heavily doping the CdTe surface is widely used (usually with Cu or Cu_2Te in order to allow tunneling transport across the interface [20]). Unfortunately, Cu is a fast migrating impurity into CdTe layer and leads to the degradation of cell efficiency [21].

*Corresponding author: santohe@solid.fizica.unibuc.ro

In this work some optical and morphological properties of thermally vacuum deposited ZnTe thin films are investigated, for further use of ZnTe thin films as additional layer for back contacts in CdTe solar cells. Experimental details on the ZnTe thin films deposition and characterization methods are given in the second section of the paper. The results are presented and discussed in the third section, while in the last section the main conclusions are summarized.

2. Experimental details

Zinc telluride thin films were deposited by thermal vacuum evaporation (TVE) using optical glass as substrates. The ZnTe powder was introduced into a quartz container (crucible) heated using an electric resistance at 550° C. The quartz crucible was covered with a quartz-wool plug in order to avoid the ZnTe powder sputtering during the deposition. The glass substrates were heated and maintained at 230° C. The distance between the evaporator (the source) and the substrates was set to 10 cm, while the pressure inside the chamber during deposition was 5×10^{-5} Torr.

After finishing the ZnTe thin films deposition, samples were subjected to a local thermal treatment performed in the same deposition chamber [22 – 25] to improve the quality of these films. The ZnTe thin films were heated (annealed) at 250° C for 20 minutes at a pressure inside the chamber of 7.5×10^{-5} Torr.

The optical characterization of the prepared ZnTe thin films was made by spectroscopic ellipsometry technique, while morphological investigations were carried out using atomic force microscopy (AFM) and scanning electron microscopy (SEM).

The ellipsometric spectra were recorded at room temperature using an UVISEL™ NIR spectroscopic phase modulated ellipsometer (PMSE) from Horiba – Jobin Yvon, in a spectral range from 250 nm to 2.1 μm with 10 nm steps. The light source used was a non-polarized Xe lamp at 75 W. The photoelastic modulator was operating at 50 kHz modulation frequency. All the values obtained for ZnTe film thicknesses using the spectroscopic ellipsometry were verified with a profilometer Veeco™ Dektak 6M.

The morphological properties of the ZnTe thin film surfaces were made using an AFM microscope from TopoMetrix™ in air, with a silicon cantilever operating in contact mode. The resonance frequency was 320 kHz for a scanning rate of 1 Hz. The morphological characterizations were completed with SEM investigations using a SEM microscope from JEOL™ with different magnifications and a level a vacuum of 10^{-7} mbar.

3. Results and discussion

The optical characterizations of deposited ZnTe semiconductor thin films were made using the spectroscopic ellipsometry technique. The experimental part consist in direct recording of the ellipsometric spectra (dependencies on the incident photon energies of two ellipsometric angles: the amplitude ratio (psi) and phase difference (del) between light waves known as “p-” and “s-” polarized light waves , one parallel (p) to the plane of incidence and the other (s) perpendicular to that plane) [26 – 28]. All the spectra were recorded at room temperature at an incidence angle on ZnTe samples of 70°. The ellipsometric configuration chosen for the phase modulator and analyzer positions was: M = 0°, respectively, A = 45° in respect with the incidence plane.

The values for ZnTe optical constants (refractive indices and extinction coefficients) were obtained indirectly by fitting the experimental (psi, del) ellipsometric spectra. In order to achieve this, an optical model had to be built using a dedicated software package DeltaPsi 2™ (this software allows also the setting for all the fitting parameters, including substrate thickness, surface roughness, etc.).

The fitting of ellipsometric spectra was made until a minimum value was reached for MSE (mean squared error). With this procedure the thicknesses of ZnTe thin films were also computed, the obtained values being compared with the values obtained by classic profilometry measurements. The dispersion relations used for the *n (E)* – the complex refractive index and *k (E)*

– the extinction coefficient were taken from the Adachi – New Forouhi (ANF) dispersion model [29].

The dependencies of the refractive indices and extinction coefficients on the incident photon wavelengths for ZnTe thin films of 120 nm thickness are shown in Figure 1.

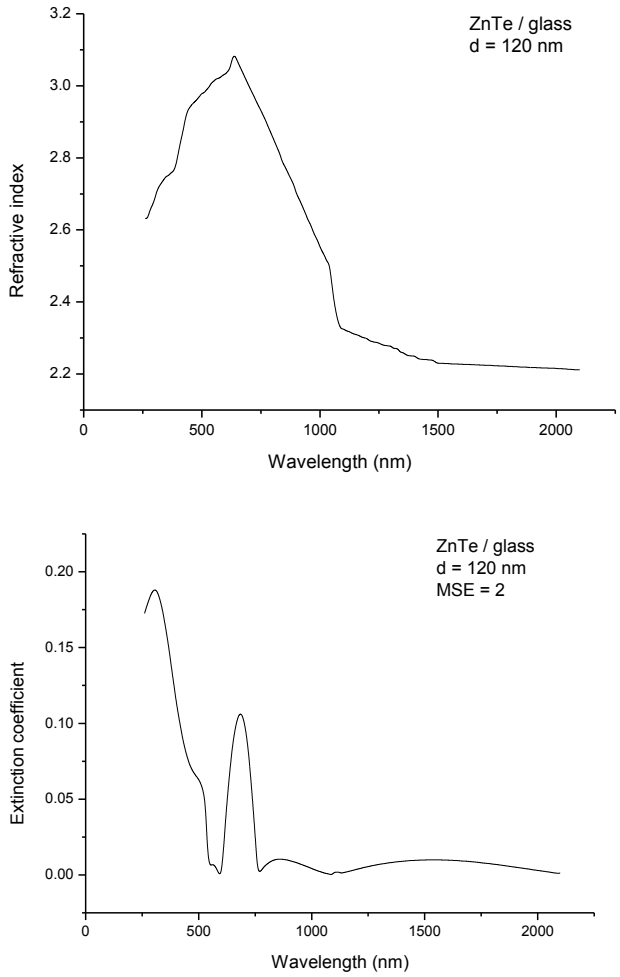

Fig. 1. Spectral dependencies of the optical constants for 120 nm thickness ZnTe thin films deposited on glass substrates

The optical constants of ZnTe thin films were computed after the mathematical fitting of the experimental ellipsometric spectra (psi, del). The fitting procedure finished when a minimum value was reached for MSE (mean squared error), respectively, MSE = 2. With this value the obtained thickness for ZnTe samples was 120 nm, in good accordance with profilometry measurements.

The variations of refractive index with photon wavelengths showed in Fig. 1 (left figure) indicates a decrease in refractive indices values with the increase of incident photon wavelengths (normal dispersion behavior) for a large spectral range. From the variations of extinction coefficient with photon wavelengths in Fig. 1 (right figure), strong light absorptions are obtained below 500 nm and especially in UV region, while the ZnTe thin films are almost perfect transparent in IR region.

In Figure 2 the transmission curve of ZnTe thin films is plotted in the same wide spectral range. The optical transmission values *T* were computed using the following formula [30]:

$$\log(\frac{1}{T}) = \frac{4\pi d k_\lambda}{2.303\lambda} \quad (1)$$

where d is thickness of the film, k_λ is the extinction coefficient calculated from the ellipsometric spectra as above mentioned and λ is the wavelength of the incident radiation.

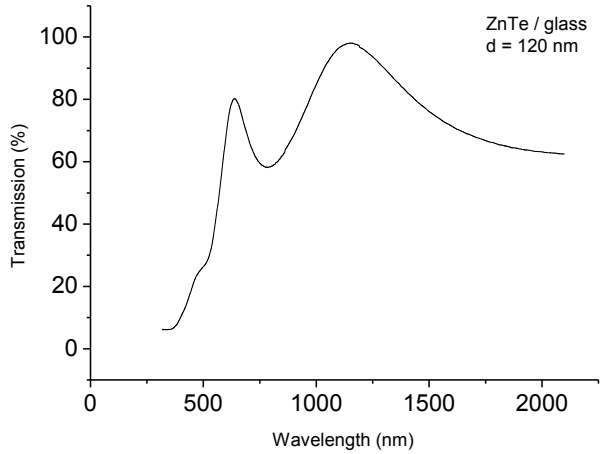

Fig. 2. The optical transmission curve for ZnTe thin films as obtained from spectroscopic ellipsometry computing

The optical transmittance curve of thermally vacuum deposited ZnTe thin films is showed in Fig. 2. It was observed that the fall of the optical transmittance at the band edge is very sharp for ZnTe thin films deposited at substrate temperatures of 230° C and this could indicate that ZnTe thin films have a good crystallinity.

The absorption coefficient (α) was calculated using the values obtained for the extinction coefficient. The formula used was [31]:

$$\alpha = \frac{4\pi k_\lambda}{\lambda} \quad (2)$$

where k_λ is the extinction coefficient and λ is the photon wavelength.

In Figure 3 the absorption spectra of ZnTe thin films is plotted against the incident photon energy.

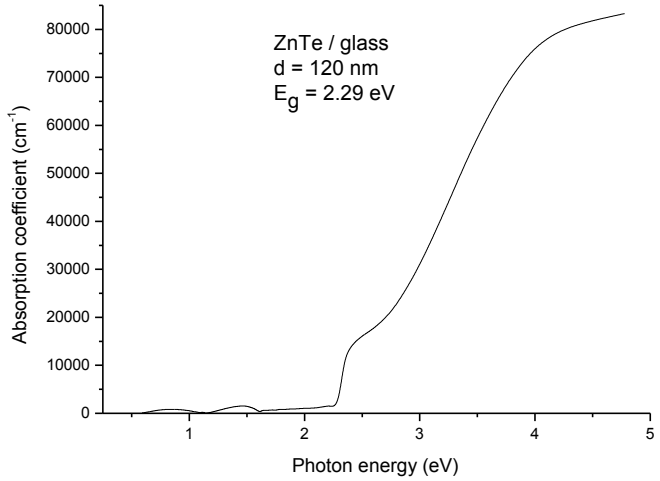

Fig. 3. Absorption spectra of ZnTe thin films deposited at 550 °C and thermally treated at 230 °C

From the Fig. 3 a sharp increase in absorption coefficient is observed at photon energies above 2.2 eV which is near the band gap region. Since ZnTe is a semiconductor material with wide direct transition type band gap, the optical band gap was obtained directly by extrapolating the square of the absorption coefficient $(\alpha h\upsilon)^2$ versus the incident photon energy ($h\upsilon$), method used also for other A2-B6 semiconducting compounds [32-35]. The obtained value for the optical band gap of ZnTe thin films using this well-known dependence is 2.29 eV, corresponding with the existing data about this semiconductor material [32].

The morphological characterizations of the surfaces corresponding to ZnTe thin films were made using AFM (Atomic Force Microscopy) and SEM (Scanning Electron Microscopy) techniques. In Figure 4 are presented both bi-dimensional and three-dimensional AFM images for thermally vacuum deposited ZnTe thin films of two different thicknesses.

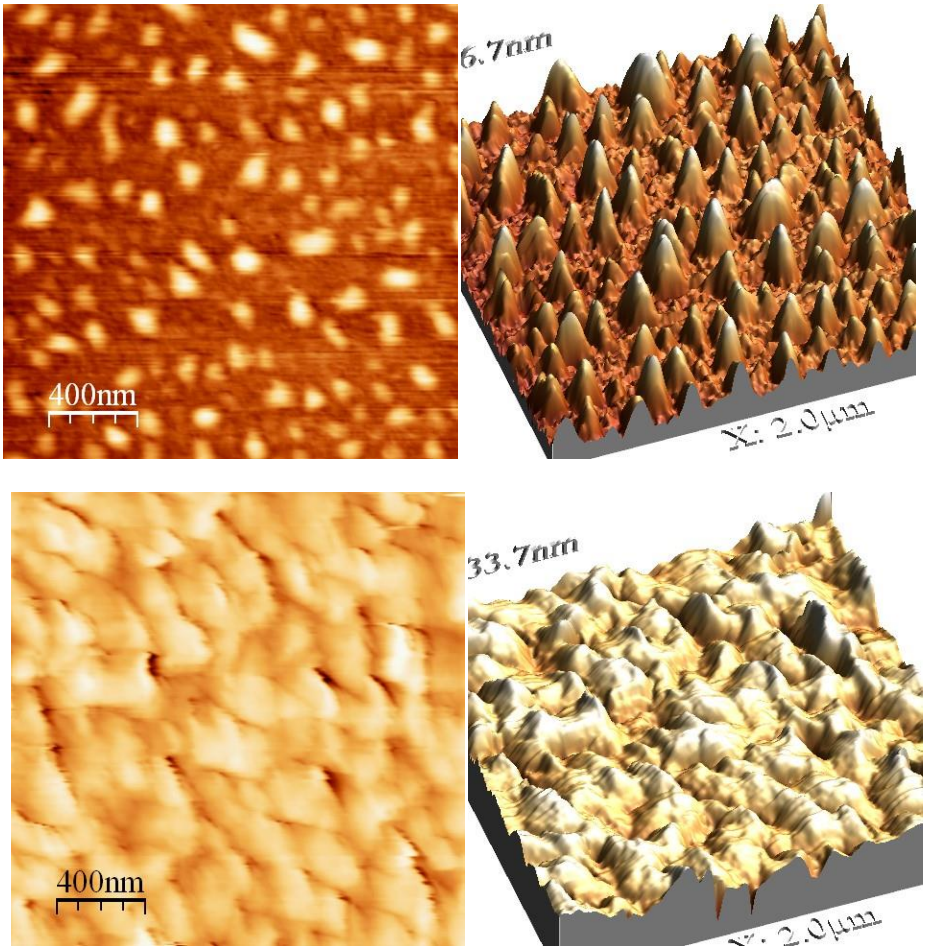

Fig. 4. Bi-dimensional (left column) and three-dimensional (right column) AFM images for ZnTe thin films of two different thicknesses: 120 nm (upper row), respectively, 600 nm (lower row)

The sampling areas used in the Fig. 4 were 2 × 2 [µm × µm]. Both investigated ZnTe samples were post-deposition thermally annealed at 250° C for 20 minutes in the same deposition chamber. Due to this thermal treatment a more uniform distribution of grains over the film surfaces was obtained.

The AFM images presented in Fig. 4 provide also quantitative data regarding the surface parameters (surface roughness, peaks distribution parameters, etc.). To achieve these data a dedicated image processing software (WSxM 4.0^{TM}) was used. In the Table 1 are showed the obtained values for the parameters used to describe the surface morphology.

Tabel 1. Surface morphology parameters for ZnTe thin films

ZnTe films thickness (nm)	Average roughness (nm)	RMS roughness (nm)	Skewness Parameter	Kurtosis parameter
120	6.7	8.27	1.16	4.25
600	33.7	44.2	0.92	5.89

As we can see from the Table 1, the ZnTe films roughness increases with the film thickness most likely due to a three – dimensional growth mechanism. Both the average roughness (1st order statistical parameter for grains height distribution) increases from 6.7 nm to 33.7 nm and the root mean square (RMS) roughness (2nd order statistical parameter for grains peaks distribution) increases from 8.27 nm to 44.2 nm, when the films thickness increases between 120 nm and 600 nm.

The investigation of the peaks distribution on the ZnTe film surfaces means also the calculus of two other statistical moments: Skewness parameter (which is a 3rd order statistical moment used to describe how symmetric a statistical distribution is) and Kurtosis parameter (which is a 4th order statistical moment used to show how sharp or how broad is that particular distribution).

From the Table 1, we can see that Skewness parameter slightly decreased from 1.16 to 0.92 with increasing the films thickness. This indicates that for the thicker ZnTe film the peaks distribution on the surface is more symmetric than for the case of thinner ZnTe film. As for the Kurtosis parameter this increase from 4.25 to 5.89 with increasing the films thickness, so a more sharp distribution of peaks was obtained for the thicker ZnTe film.

Morphological investigations of ZnTe film surfaces were continued using a SEM microscope. To obtain the SEM images the electron acceleration voltage was set to 3 kV (corresponding to a magnification of × 40000) and with the focal length set at 15 mm.

In Figure 5 are showed SEM images corresponding for the same ZnTe samples as those investigated by AFM.

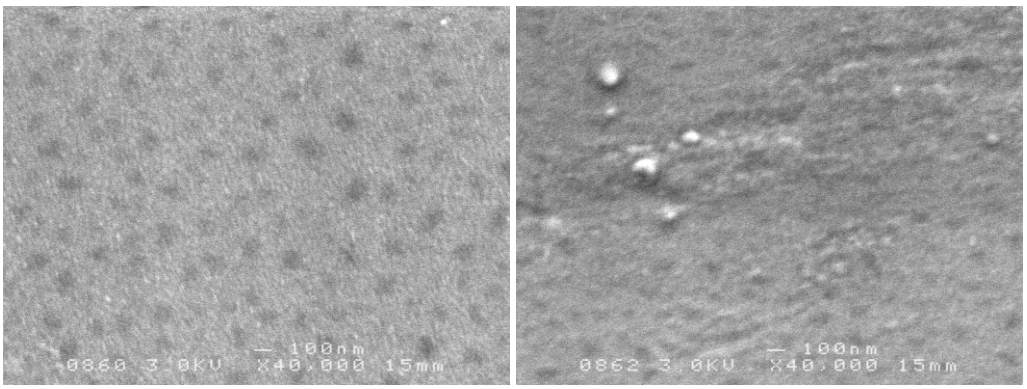

Fig. 5. SEM images for ZnTe thin films of two different thicknesses: 120 nm (left image), respectively, 600 nm (right image)

From the Fig. 5 we observe that both ZnTe films of different thicknesses have a grain-like kind of surface morphology. Also, despite some irregularities caused by manipulations during SEM investigations for the case of the thicker ZnTe sample, we can see that ZnTe samples have smooth surfaces thanks to the post-deposition thermal treatments applied.

4. Conclusions

ZnTe thin films of different thicknesses were deposited by TVE (thermal vacuum evaporation) using optical glass as substrates. The optical constants (refractive indices, extinction coefficients, optical transmittances, absorption coefficients and optical band gap) were computed using spectroscopy ellipsometry (SE) technique. Despite the fact that spectroscopic ellipsometry is an indirect optical investigation technique, the obtained results for the optical constants of ZnTe thin films are in good agreement with previous results. Morphological investigations of ZnTe film surfaces carried out using AFM and SEM techniques proved that ZnTe films have well defined grains and their distributions along the surfaces for different thicknesses were discussed. Both AFM and SEM images showed that ZnTe film surfaces are uniform. It is concluded that the film surfaces become more dense, uniform and compact after the applied thermal treatment.

Acknowledgements

Authors wish to thank to Romain Mallet and Guillaume Mabillau from SCIAM, Angers, France for AFM and SEM characterizations. This work was supported by the Program-PN II developed by MEN-UEFISCDI, Project Nr.288/2014.

References

[1] N. Nakayama, S. Itoh, H. Okuyama, M. Ozawa, T. Ohata, K. Nakano, M. Ikeda, A. Ishibashi, Y. Mori, Electron. Lett., **29**(25), 2194 (1993).
[2] A. Erlacher, A. R. Lukaszew, H. Jaeger, B. Ullrich, Surf. Sci., **600(**18), 3762 (2006).
[3] N. Amin, K. Sopian, M. Konagai, Sol. Energ. Mat. Sol. C., **91**, 1202 (2007).
[4] H. Y. Chao, J. H. Cheng, J. Y. Lu, Y. H. Chang, C. L. Cheng, Y. F. Chen, Superlattice Microst., **47**, 160 (2010).
[5] S. H. Lee, A. Gupta, S. L. Wang, A. D. Compaan, B. E. McCandless, Sol. Energ. Mat. Sol. C., **86,** 551 (2005).
[6] S. Bhumia, P. Bhattacharya, D. N. Bose, Mater. Lett., **27**, 307 (1996).
[7] D. Zeng, W. Jie, H. Zhou, Y. Yang, Thin Solid Films, **519**, 4158 (2011).
[8] A. A. Ibrahim, Vacuum, **81**, 527 (2006).
[9] J. Pattar, S. N. Sawant, M. Nagaraja, N. Shashank, K. M. Balakrishna, H. M. Mahesh, Int. J. Electrochem. Sc., **4**, 369 (2009).
[10] G. G. Rusu, M. Rusu, M. Girtan, Vacuum, **81**, 1476 (2007).
[11] T. Barona, K. Saminadayarb, N. Magnea, J. Appl. Phys., **83**, 1354 (1998).
[12] A. M. Salem, T. M. Dahy, Y. A. El-Gendy, Physica B, **403**, 3027 (2008).
[13] O. de Melo, E. M. Larramendi, J. M. Duart, M. H. Velez, J. Stangl, H. Sitter, J. Cryst. Growth, **307**, 253 (2007).
[14] V. S. John, T. Mahalingam, J. P. Chu, Solid State Electron., **49**, 3 (2005).
[15] K. R. Murali, M. Ziaudeen, N. Jayaprakash, Solid State Electron., **50**, 1692 (2006).
[16] L. Feng, L. Wu, Z. Lei, W. Li, Y. Cai, W. Cai, J. Zhang, Q. Luo, B. Li, J. Zheng, Thin Solid Films, **515**, 5792 (2007).
[17] J. Sites, J. Pan, Thin Solid Films, **515**, 6099 (2007).
[18] O. Toma, L. Ion, M. Girtan, S. Antohe, Solar Energy, **108**, 51 (2014).
[19] M. A. Green, K. Emery, Y. Hishikawa, W. Warta, E. D. Dunlop, Prog. Photovoltaic. Res. Appl., **21**, 827 (2013).
[20] C. R. Corwine, A. O. Pudov, M. Gloeckler, S. H. Demtsu, J. R. Sites, Sol. Energ. Mat. Sol. C., **82**, 481 (2004).
[21] N. Romeo, A. Bosio, A. Romeo, Sol. Energ. Mat. Sol. C., **94**, 2 (2010).
[22] S. Antohe, L. Ion, M. Girtan, O. Toma, Rom. Rep. Phys., **65(**3), 805 (2013).

[23] O. Toma, R. Pascu, M. Dinescu, C. Besleaga, T. L. Mitran, N. Scarisoreanu, S. Antohe, Chalcogenide Lett., **8(**9), 541 (2011).
[24] S. Antohe, V. Ghenescu, S. Iftimie, A. Radu, O. Toma, L. Ion, Dig. J. Nanomater. Bios. **7**(3), 941 (2012).
[25] O. Toma, S. Iftimie, C. Besleaga, T. L. Mitran, V. Ghenescu, O. Porumb, A. Toderas, M. Radu, L. Ion, S. Antohe, Chalcogenide Lett., **8(**12), 747 (2011).
[26] R. M. A. Azzam, N. M. Bashara, Ellipsometry and Polarized Light, North-Holland, Amsterdam (1977).
[27] H. G. Tompkins, A. W. McGahan, Spectroscopic Ellipsometry and Reflectometry: A User's Guide, John Wiley & Sons, New York (1999).
[28] H. Fujiwara, Spectroscopic Ellipsometry – Principles and Applications, John Wiley & Sons, London (2007).
[29] H. Yoshikawa, S. Adachi, Jpn. J. Appl. Phys. **36**, 6237 (1997).
[30] S. Lalitha, R. Sathyamoorthy, S. Senthilarasu, A. Subbarayan, K. Natarajan, Sol. Energ. Mat. Sol. C., **82**, 187 (2004).
[31] S. Antohe, L. Ion, M. Girtan, O. Toma, Rom. Rep. Phys., **65(**3), 805 (2013).
[32] A. Mondal, S. Chaudhuri, A. K. Pal, Appl. Phys. A – Mater., **43**, 81 (1987).
[33] L. Ion, I. Enculescu, S. Iftimie, V. Ghenescu, C. Tazlaoanu, C. Besleaga, T. L. Mitran, V. A. Antohe, M. M. Gugiu, S. Antohe, Chalcogenide Lett.**7**(8), 521 (2010)
[34] S. Antohe, L. Ion, V.A. Antohe, M. Ghenescu, H. Alexandru, J. Optoelectron. Adv. Mater. **9(**5), 1382 (2007).
[35] L. Ion, V. Ghenescu, S. Iftimie, V. A. Antohe, A. Radu, M. Gugiu, G. Velisa, O. Porumb, S. Antohe, Optoelectronics and Advanced Materials-Rapid Communications, **4**(8), 1114 (2010)